Understanding the cause of suppressed void swelling in additively manufactured steels

Alec Pfundheller, Advisor: Lin Shao

Department of Nuclear Engineering

Texas A&M University

ETI Annual Workshop

February 20 – 21, 2024, Golden, CO

AM Roadmaps by EPRI

Two Roadmaps have been developed by EPRI

– Primary pressure boundary Roadmap

– Reactor Internals Roadmap

- Roadmaps are focused on LWRs, ALWRs and SMRs
- Roadmap development generated based on component **size/materials**

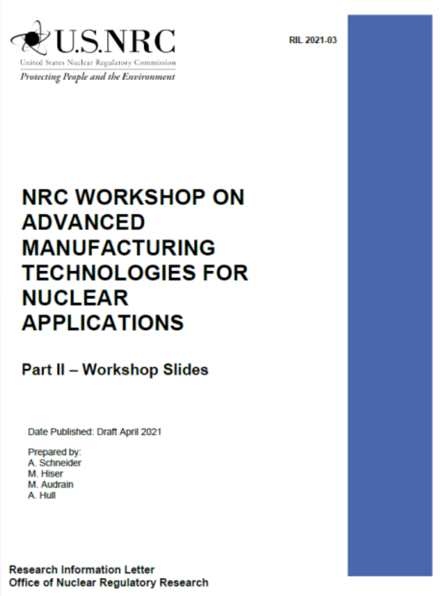

U.S.NRC
United States Nuclear Regulatory Commission
Protecting People and the Environment

RIL 2021-03

NRC WORKSHOP ON ADVANCED MANUFACTURING TECHNOLOGIES FOR NUCLEAR APPLICATIONS

Part II – Workshop Slides

Date Published: Draft April 2021

Prepared by:
A. Schneider
M. Hiser
M. Audrain
A. Hull

Research Information Letter
Office of Nuclear Regulatory Research

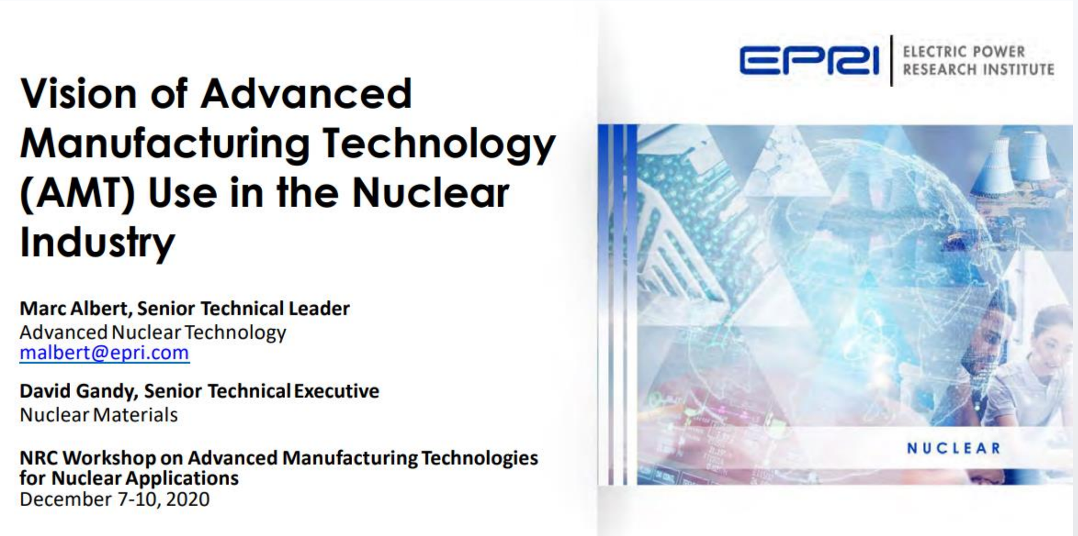

Vision of Advanced Manufacturing Technology (AMT) Use in the Nuclear Industry

Marc Albert, Senior Technical Leader
Advanced Nuclear Technology
malbert@epri.com

David Gandy, Senior Technical Executive
Nuclear Materials

NRC Workshop on Advanced Manufacturing Technologies for Nuclear Applications
December 7-10, 2020

EPRI ELECTRIC POWER RESEARCH INSTITUTE

NUCLEAR

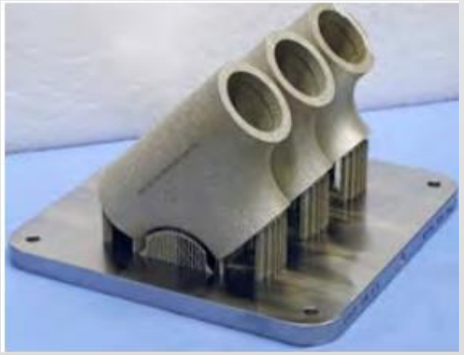

Laser Powder Bed Fusion
<75 lbs

Direct Energy Deposition
<500 lbs

Powder Metallurgy - HIP Hot Isostatic Pressing
100 to 10,000 lbs

National Nuclear Security Administration

AM Roadmaps by EPRI

AM Roadmap

EPRI Report: 3002018276

- Material Development and ASME Code Case Priorities
  - AM Marketplace Materials
  - Non-AM Marketplace Materials
  - Feedstock Quality Guidelines
  - Fatigue Data
  - SCC and Irradiation Data
- Process Related Gaps
  - ASME PTB Guideline for DED
  - Industry consensus regarding minimum essential parameters for each AM process
  - Heat Treatment Effects (HIP and SA)
- Non-Destructive Examination Related Gaps
  - Technical Basis for Defect Acceptance Criteria
  - NDE Improvements for AM Parts
  - Guidelines for NDE of DED Parts
  - In-situ Real-Time Build Health Monitoring
- Recommended Practices for Purchases AM Parts

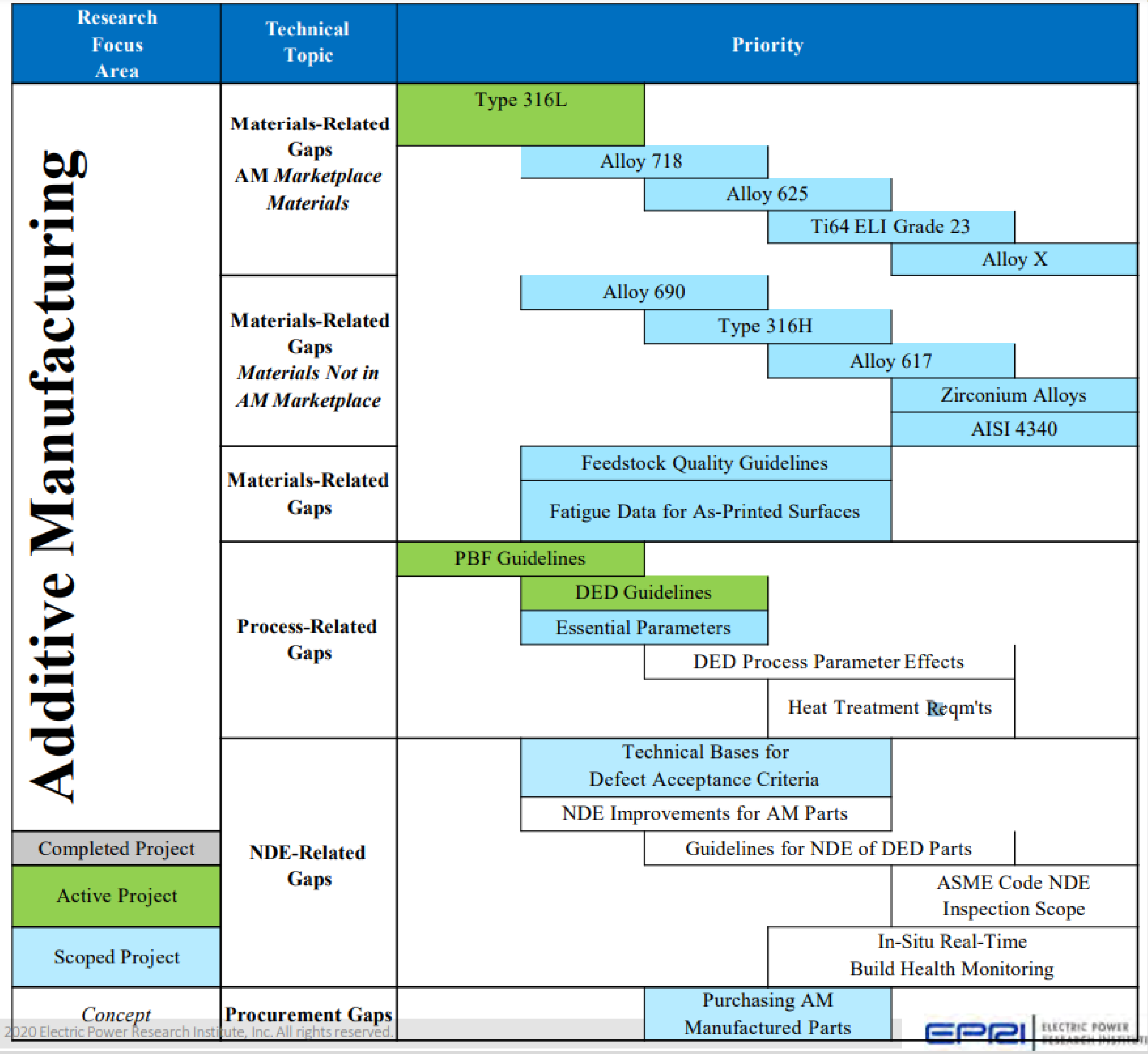

 www.epri.com

From Marc Albert, David Gandy, NRC Workshop on Advanced Manufacturing Technologies for Nuclear Applications, 2020

Key Question

Our goal is to achieve additive manufactured stainless steels with microstructures and properties that closely resemble those of conventionally manufactured counterparts.

However, is it possible that additive manufacturing can offer unique advantages and property enhancements in reactor environments that surpass those of conventionally manufactured materials?

Journal of Nuclear Materials 566, 153739 (2022)
Journal of Nuclear Materials 546, 152745 (2021)
Materials & Design 294, 109644 (2021)

Our project had led to the following findings

- Atomic scale segregation (nanopatterned segregation in AM alloys)
- Localized phase changes around pores in AM alloys
- Boundary segregation (HAGB and cell walls in AM alloys)
- Deformation mechanism changes (dislocation gliding changes to twinning after irradiation)
- Swelling (AM alloys swell less)

- The cause was not fully understood (can be attributed to grain size, GB, dislocations, stress, impurities)
- The swelling at low dpa (<1 dpa) and low dpa rate ($<1\times10^{-4}$ dpa/s) need to investigated (considering the high sensitivity of void nucleation to dpa rate)

2 MeV proton irradiation of wrought and AM 316L

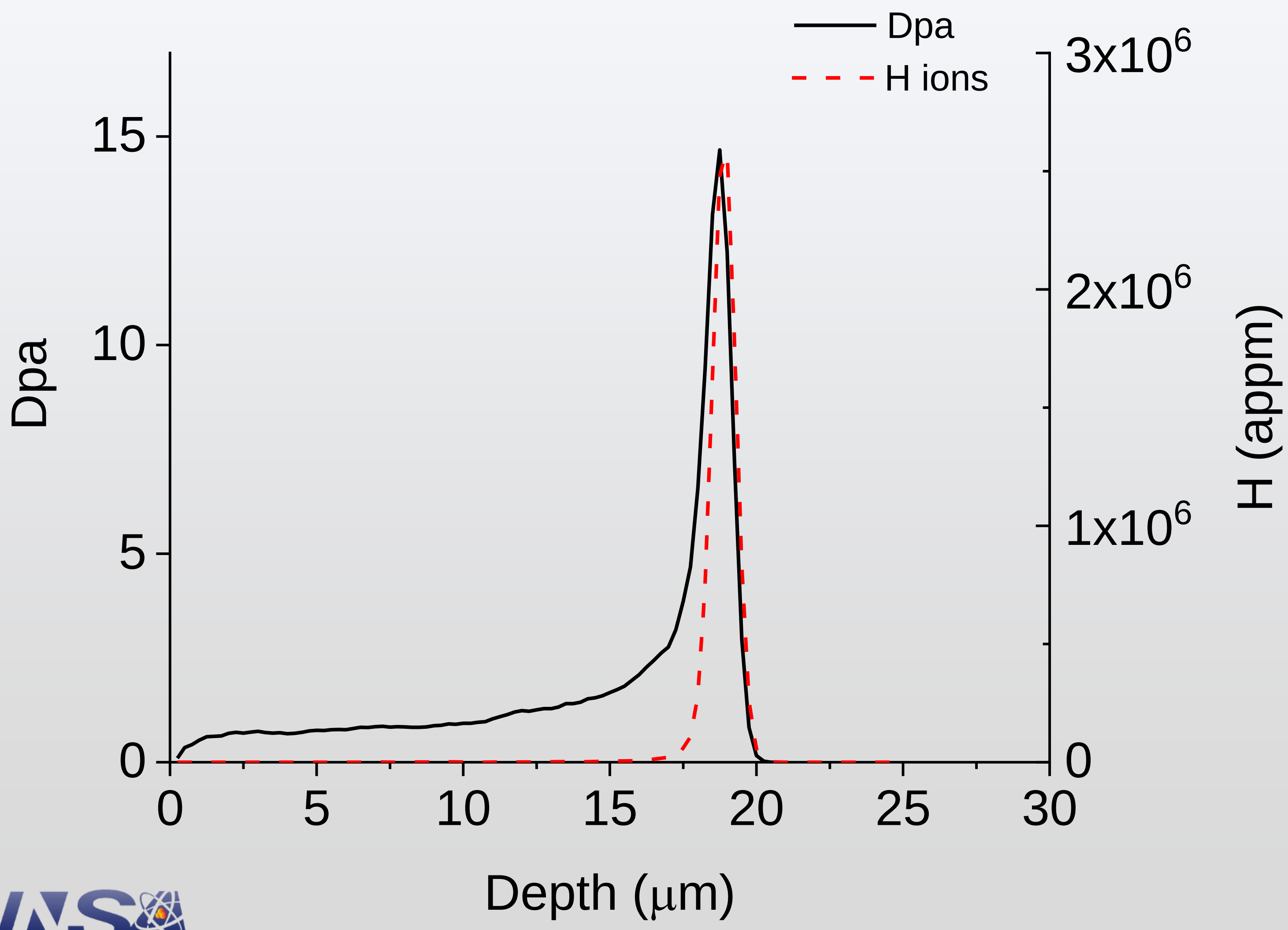

2 MeV proton irradiation creates a damage layer ~20 micron deep.

Sufficient for void swelling analysis
Sufficient for cross sectional micropillar compression testing

Other benefits of proton irradiation:

- No injected interstitial effect (different from heavy ion irradiation)
- The effect of hydrogen is very local, and the effect can be easily excluded in the data analysis

Post-irradiation characterization requires skillful FIB process

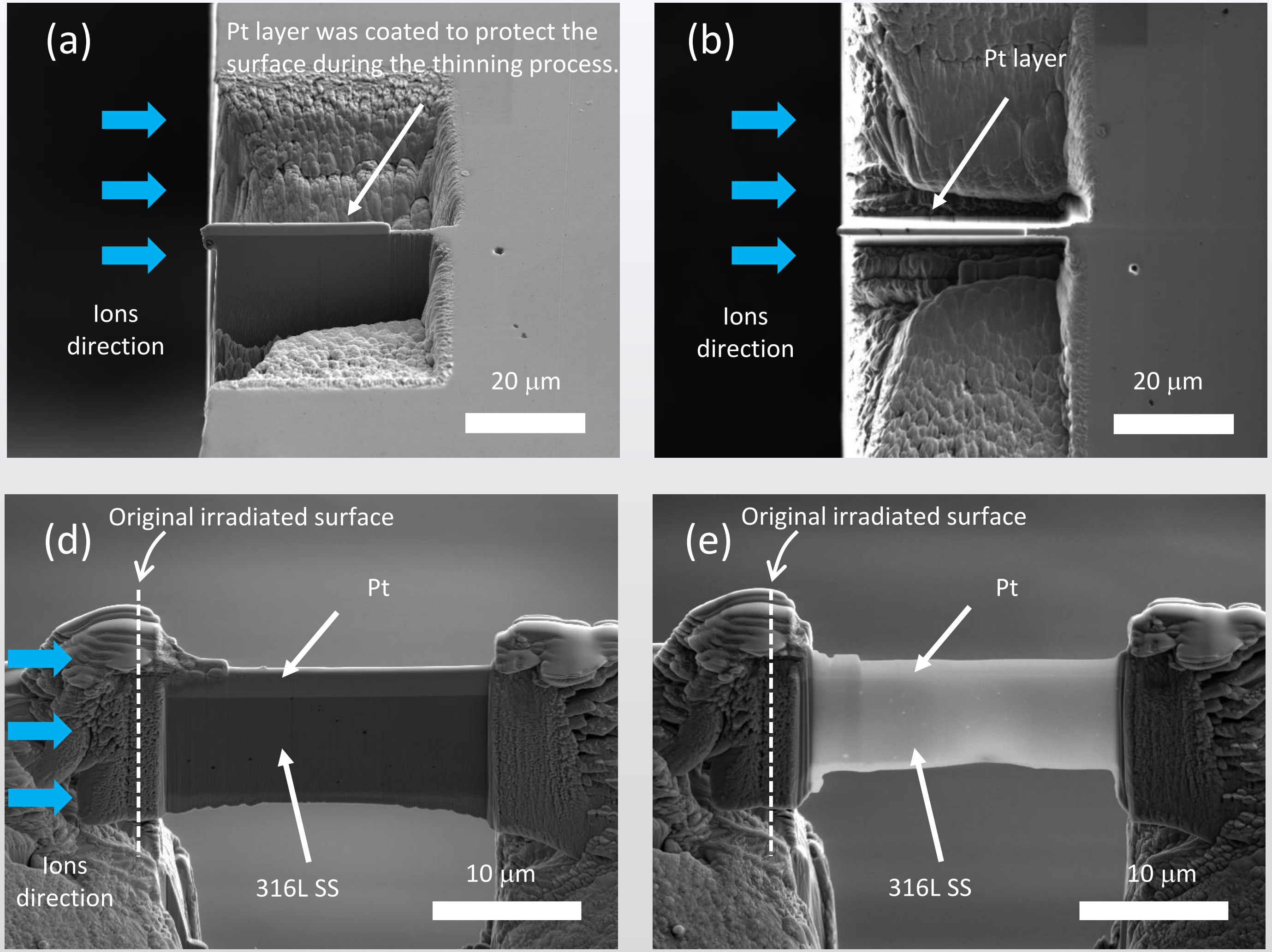

In order to extract swelling vs. local dpa, FIB is required to prepare a single TEM specimen > 20 micron in width

Swelling in wrought 316L

Surface – 300 nm | 300 nm – 900 nm | 900 nm – 1.5 um | 1.5 um – 2.1 um | 2.1 um – 2.7 um

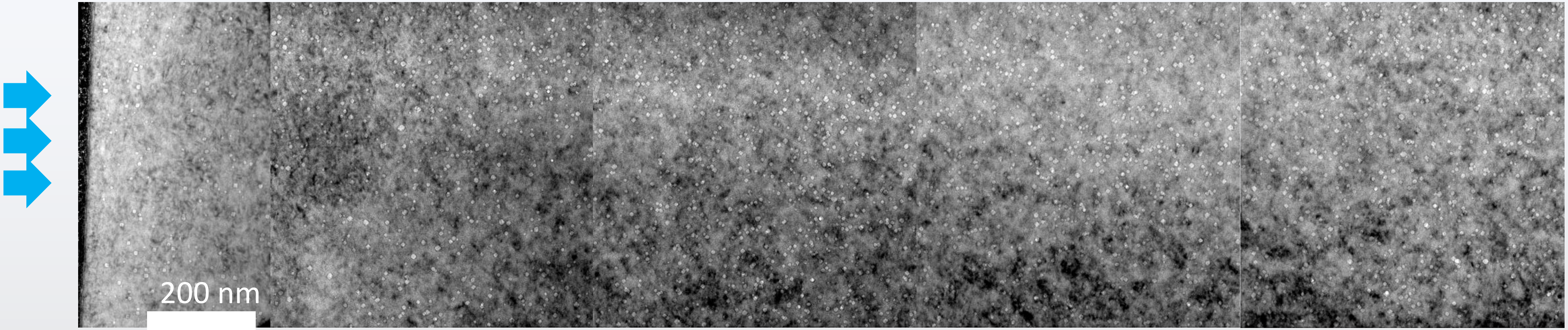

2.7 um – 3.3 um | 3.3 um – 3.9 um | 3.9 um – 4.5 um | 4.5 um – 5.1 um

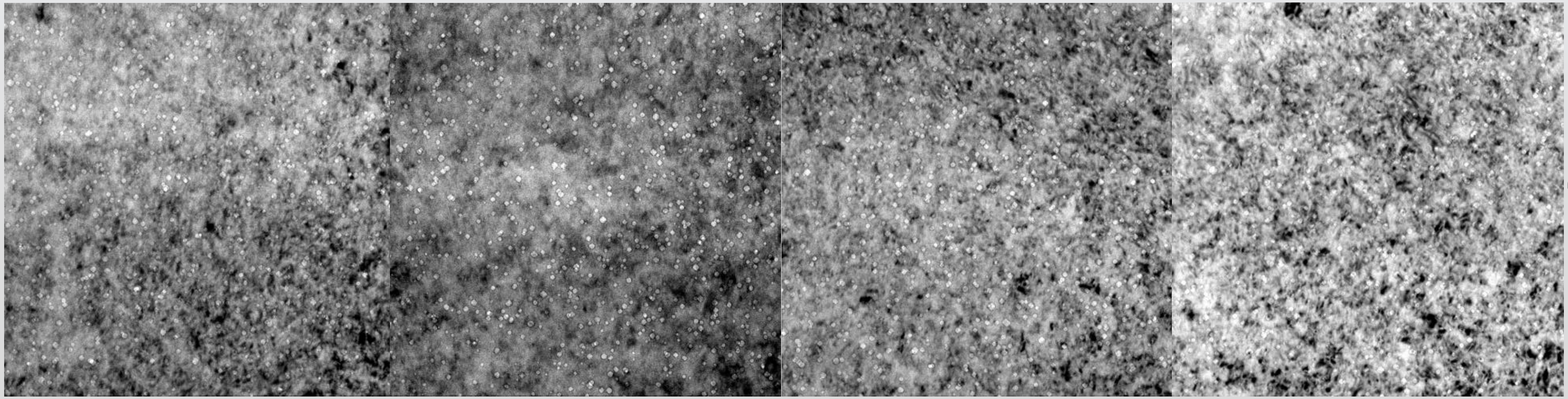

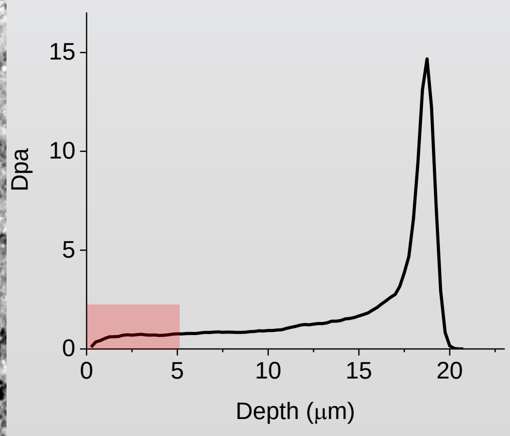

Swelling in wrought 316L

4.7 um – 5.3 um | 5.3 um – 5.9 um | 6.1 um – 6.7 um | 6.7 um –7.3 um | 7.3 um –7.9 um

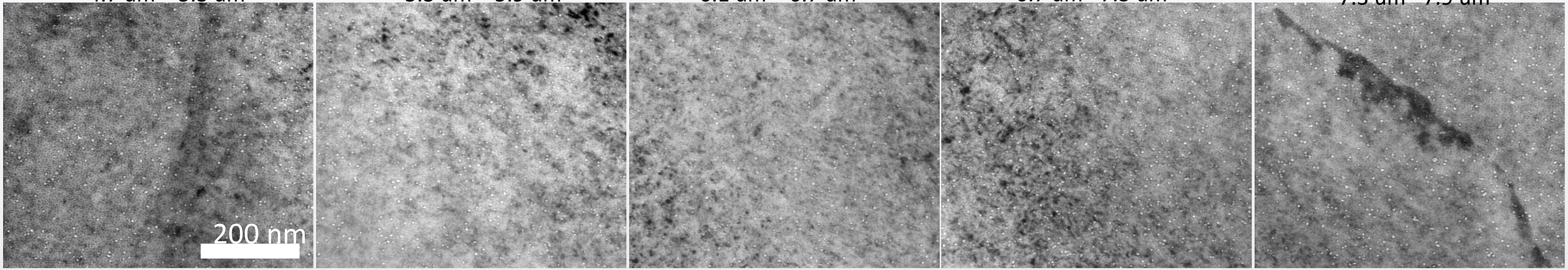

7.9 um –8.5 um | 8.5 um –9.1 um | 9.1 um –9.7 um

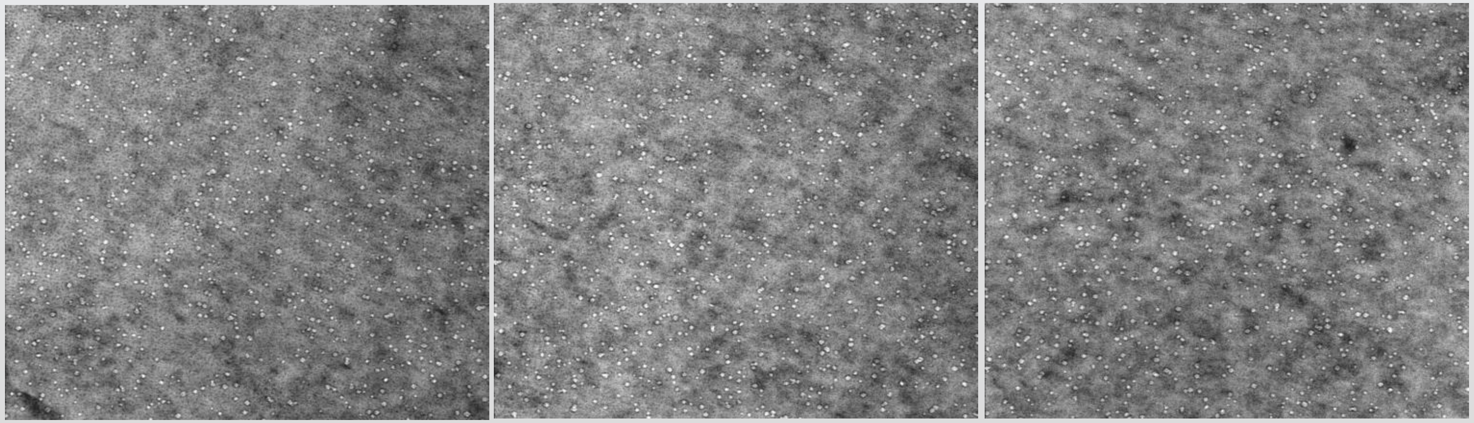

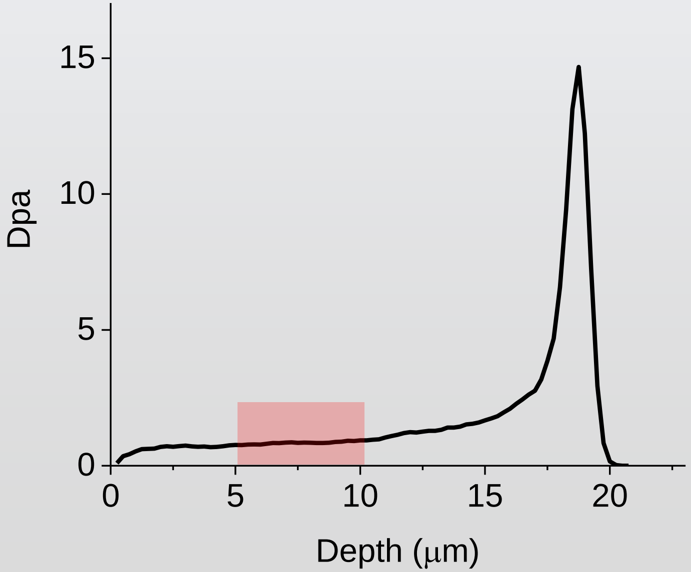

Swelling in wrought 316L

9.7 um –10.3 um

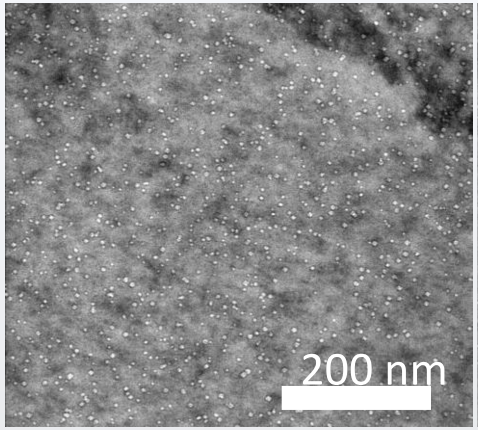

10.3 um –10.9 um

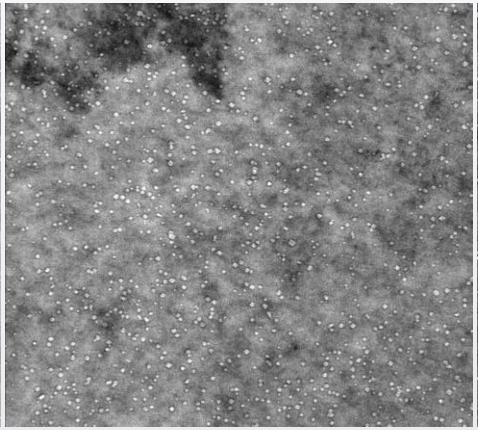

10.9 um –11.5 um

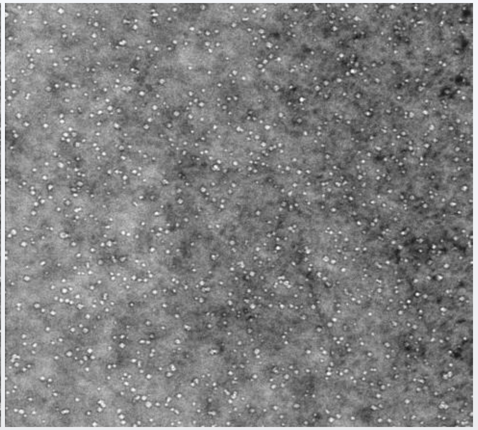

11.5 um –12.1 um

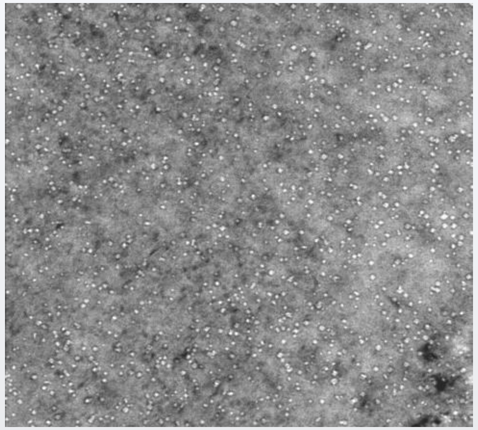

11.7 um –12.3

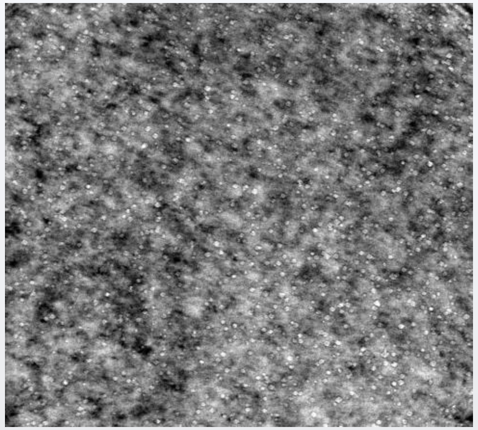

12.3 um –12.9 um

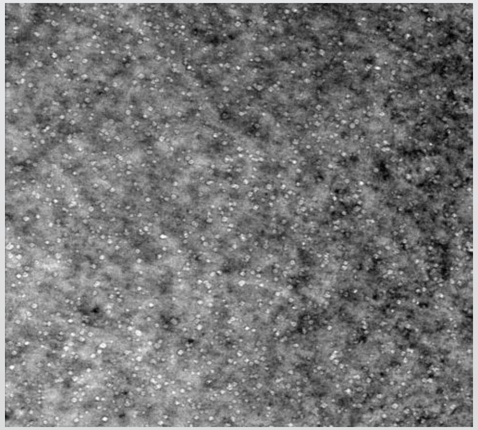

12.9 um –13.5 um

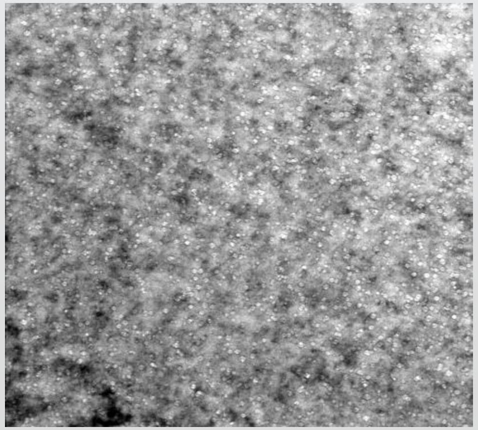

13.5 um –13.9 um

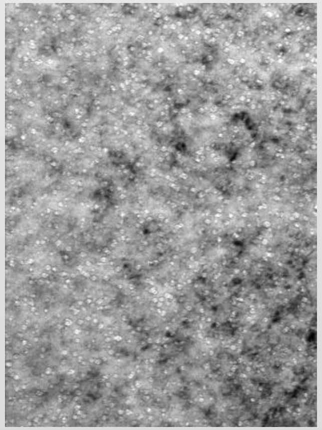

13.9 um –14.5 um

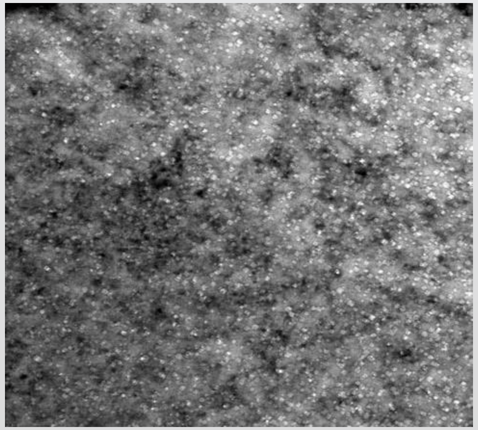

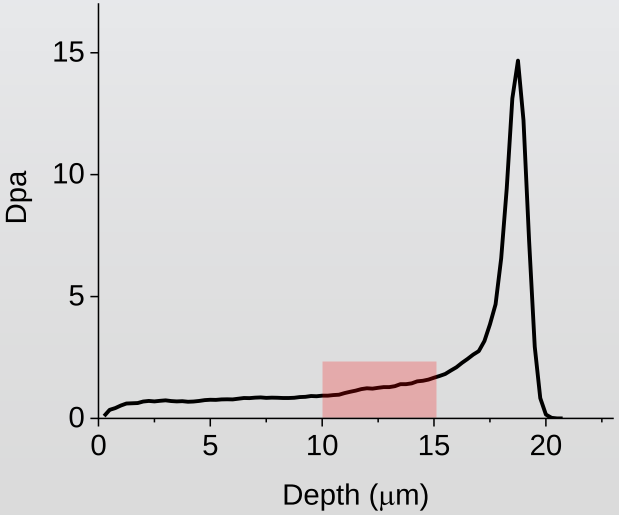

Swelling in wrought 316L

14.3 um –14.9 um 14.9 um –15.5 um 15.5 um –16.1 um 16.1 um –16.7 um

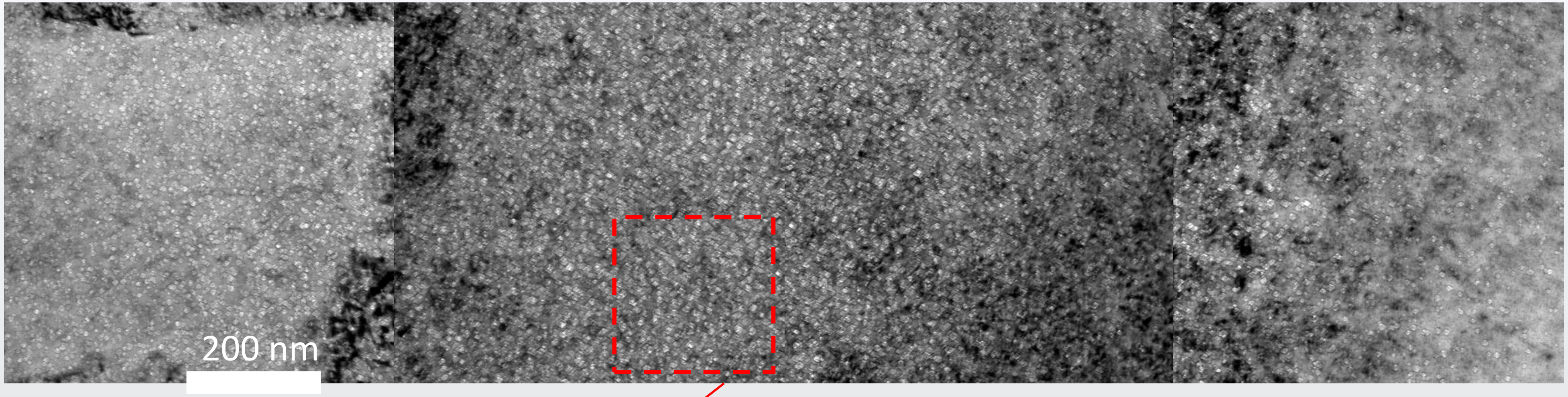

15.3 um –15.5 um

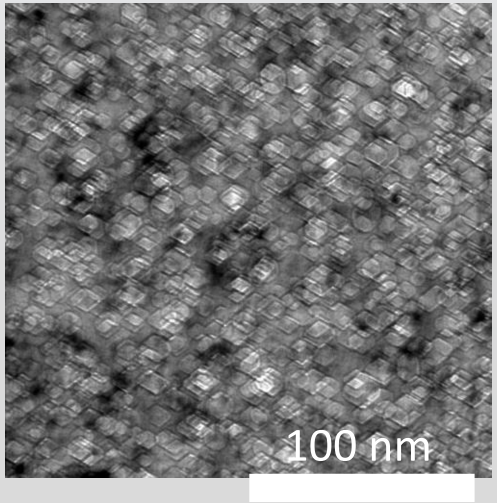

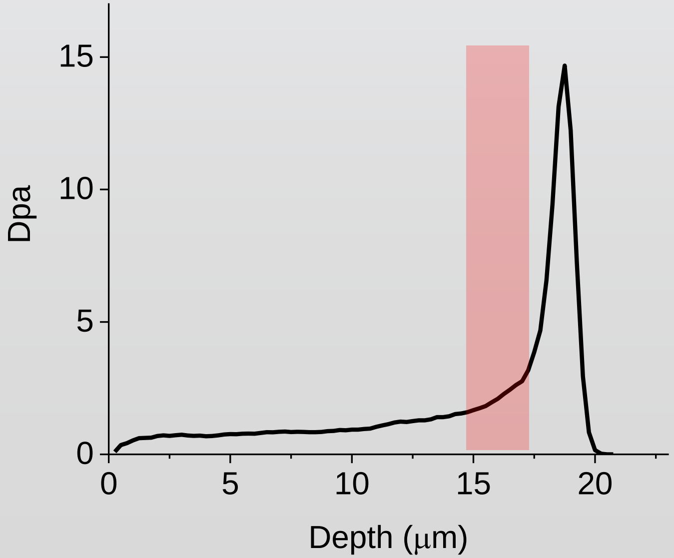

Comparison of wrought and AM 316L

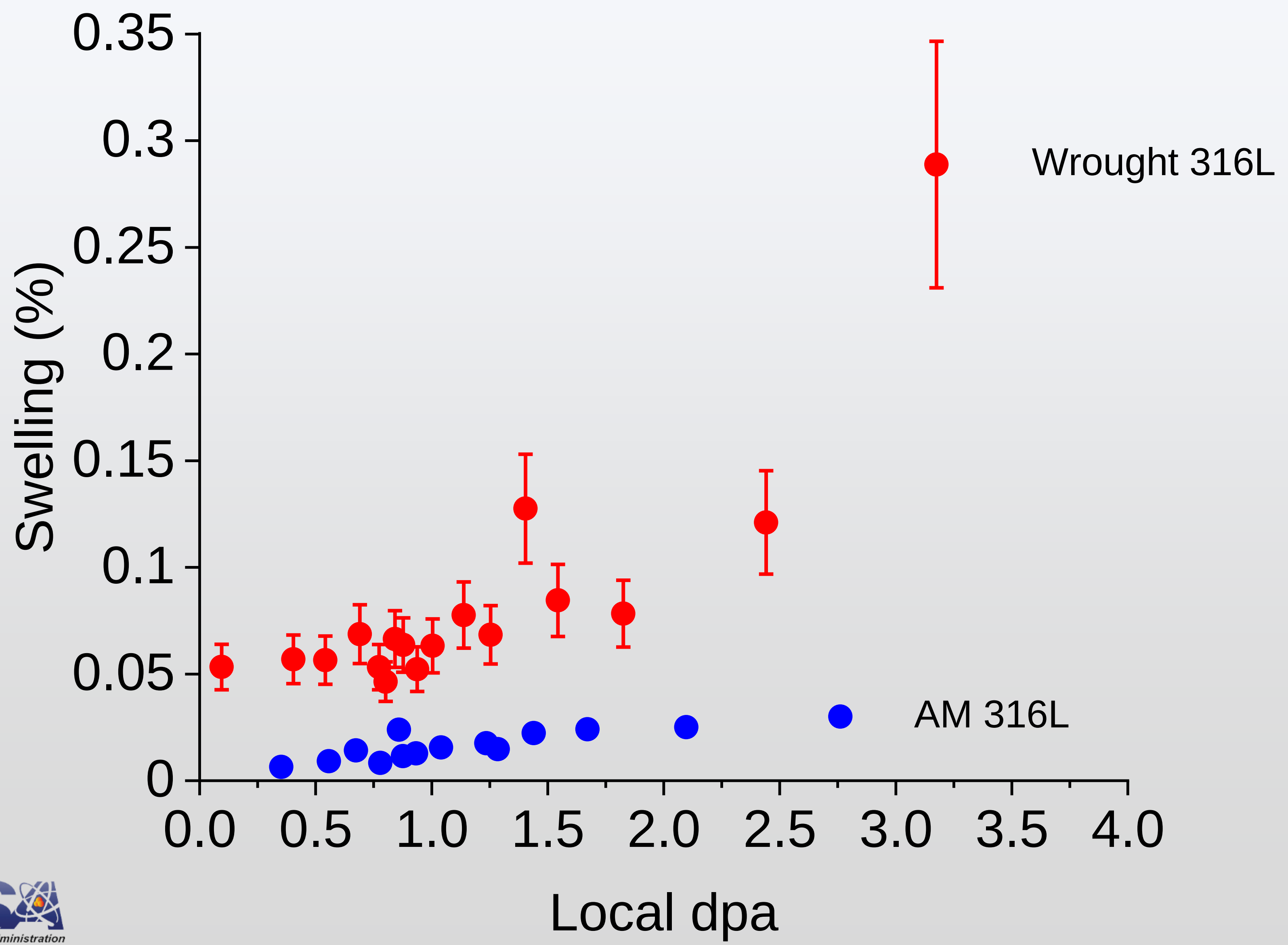

AM 316L has much more swelling resistance.

This could be caused by the difference in
- Grain
- Grain boundary
- Precipitation
- Dislocations
- Impurity

Calculations of void nucleation rates in defect supersaturated Fe

$$\frac{\partial C_v}{\partial t} = f_{survive} N K_0 + K_v^{th} - K_{\perp(v)} \rho_v C_v - K_{iv} C_v C_i + \nabla D_v \nabla C_v$$

$$\frac{\partial C_i}{\partial t} = f_{survive} N K_0 + K_i^{th} - K_{\perp(i)} \rho_i C_i - K_{iv} C_v C_i + \nabla D_i \nabla C_i$$

t – time.
$f_{survive}$ – the survival fraction of defects after the initial damage creation.
N – the atomic density of Fe.
K_0 – displacements-per-atom.
K_v^{th} and K_i^{th} – rates of vacancies and interstitials through thermal generation, respectively.
$K_{\perp(v)}$ and $K_{\perp(i)}$ – sink strength for vacancies and interstitials, respectively.
ρ_v and ρ_i – sink densities for vacancies and interstitials, respectively.
K_{iv} – the interstitial-vacancy recombination rate.
D_v and D_i – diffusivities of vacancies and interstitials, respectively.

Defect supersaturation ratios are used to calculate void nucleation rates,
using homogenous void nucleation theory (Katz, Wiedersich, Russel 1971, Lin Shao 2024)

$$J = \left[\sum_{x=1}^{x=\infty} \frac{1}{\beta_v s(x) n(x)}\right]^{-1}$$

where $s(x)$ is the surface area of a void with size x, $n(x)$ is a specific void size distribution satisfying J =0. β_v is vacancy flux to a void surface.

National Nuclear Security Administration

Calculations of void nucleation rates in defect supersaturated Fe

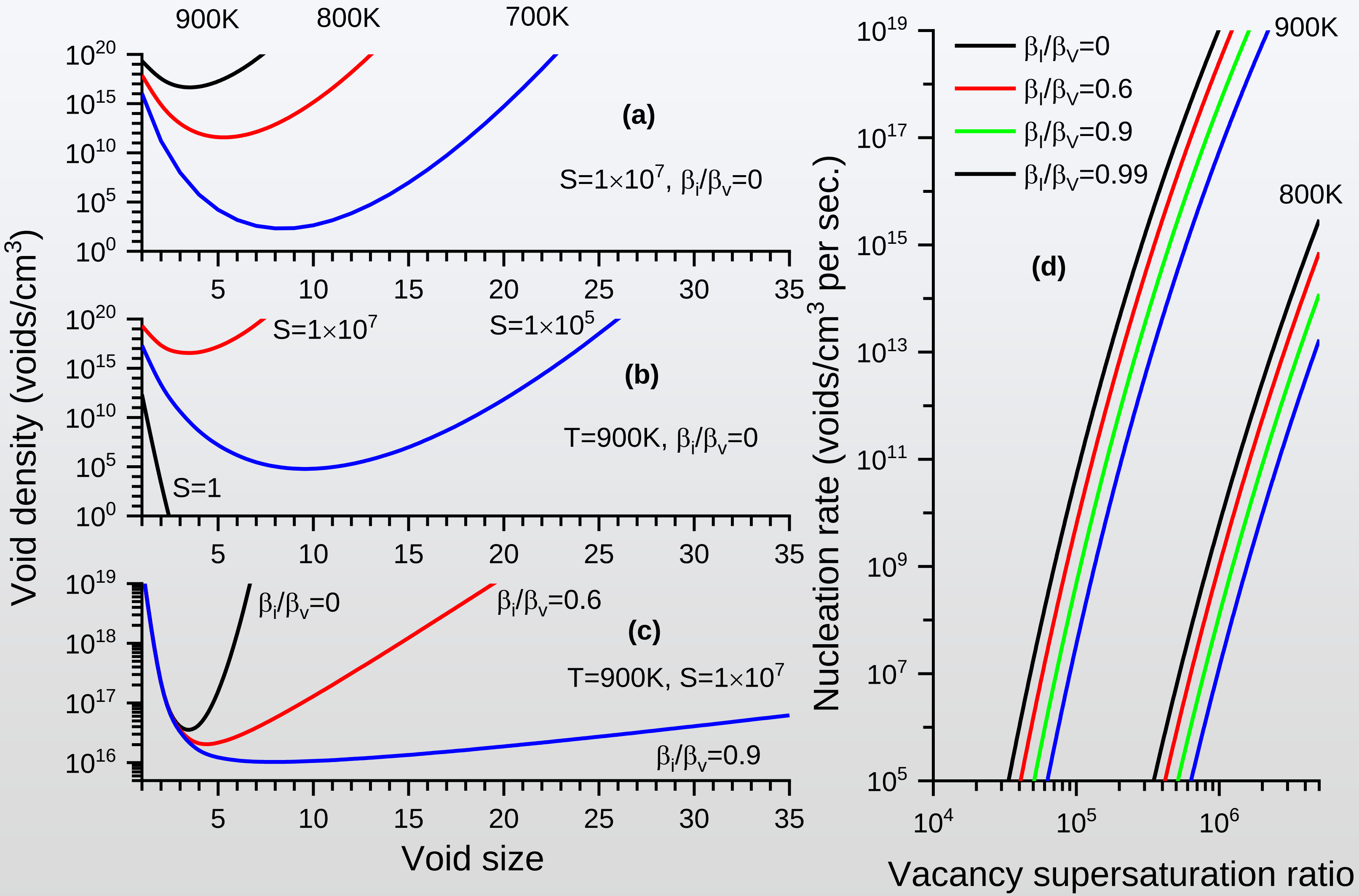

Void density under steady state void nucleation depends on

- Temperature (T)
- Vacancy supersaturation ratio (S)
- Ratio of interstitial flux to vacancy flux (β_i/β_v)

Void nucleation rates also depend on T, S, β_i/β_v

Effect of carbon on vacancy diffusivity

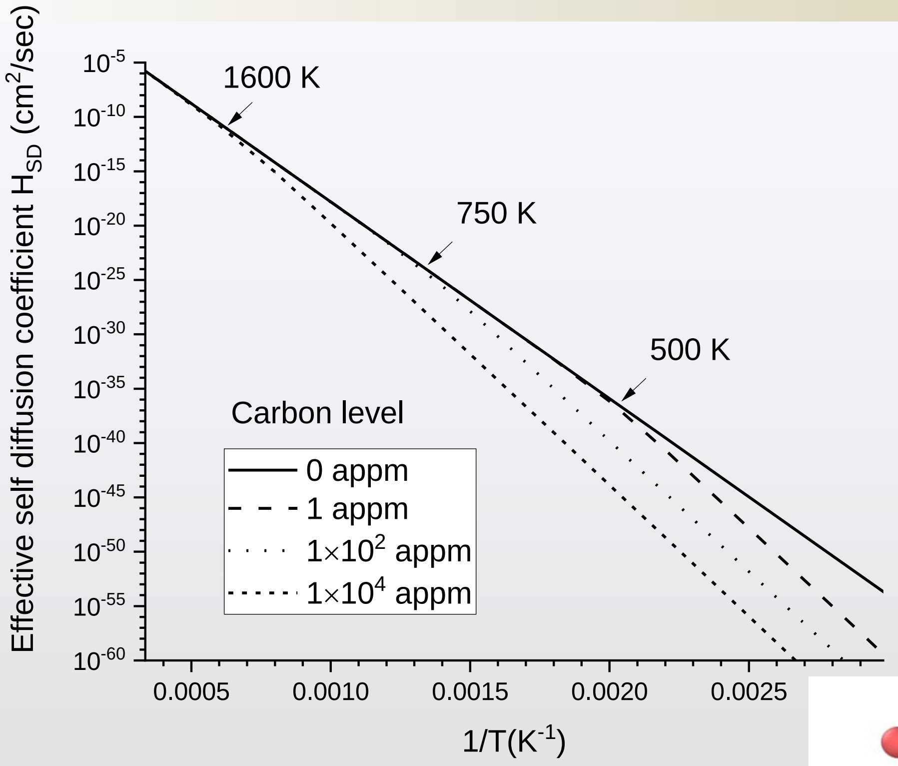

Effective vacancy diffusivity as a function of temperatures and C concentrations in α-iron.

- Diffusivity reduction results from the trapping of vacancies by carbon.
- The effect is more pronounced at low temperatures.
- The effect diminishes at high temperatures when the vacancy-carbon complex easily dissociates.
- The reduction in diffusivity increases with higher carbon concentrations.

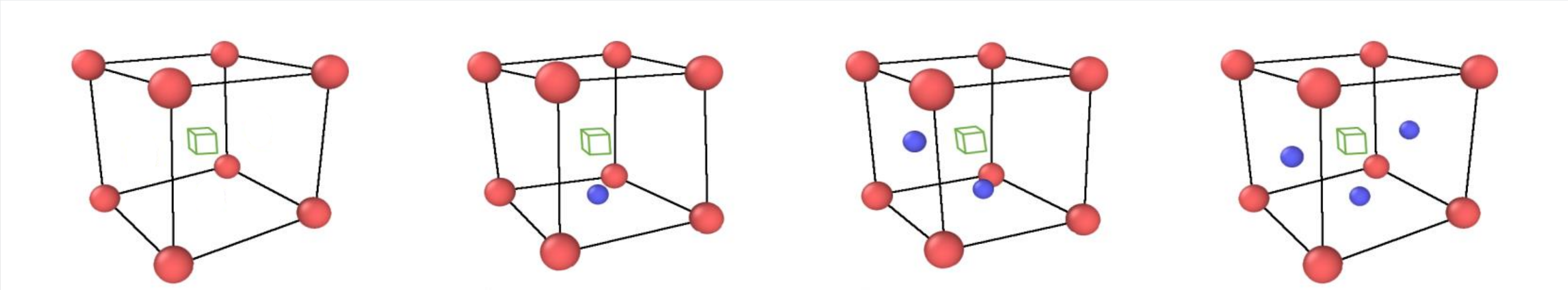

	V	VC	VC_2	VC_3
Effective vacancy migration energy	0.67 eV	1.08 eV	1.85 eV	1.97 eV

Effect of carbon on void nucleation

The map of void nucleation rates as a function of C concentrations and temperatures.

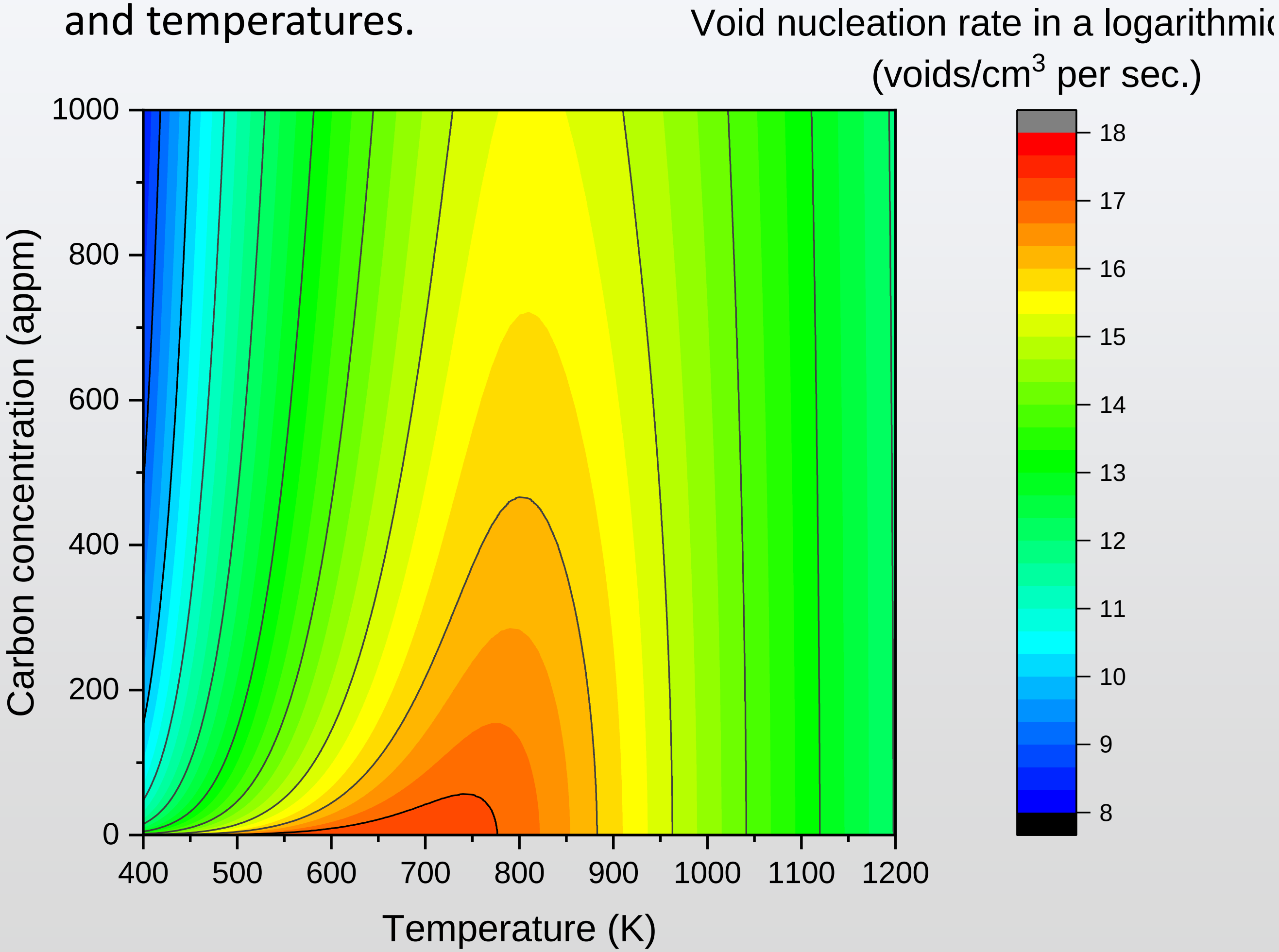

The plot of void nucleation rates as a function of temperature for C concentrations ranging from 0 to 1000 appm.

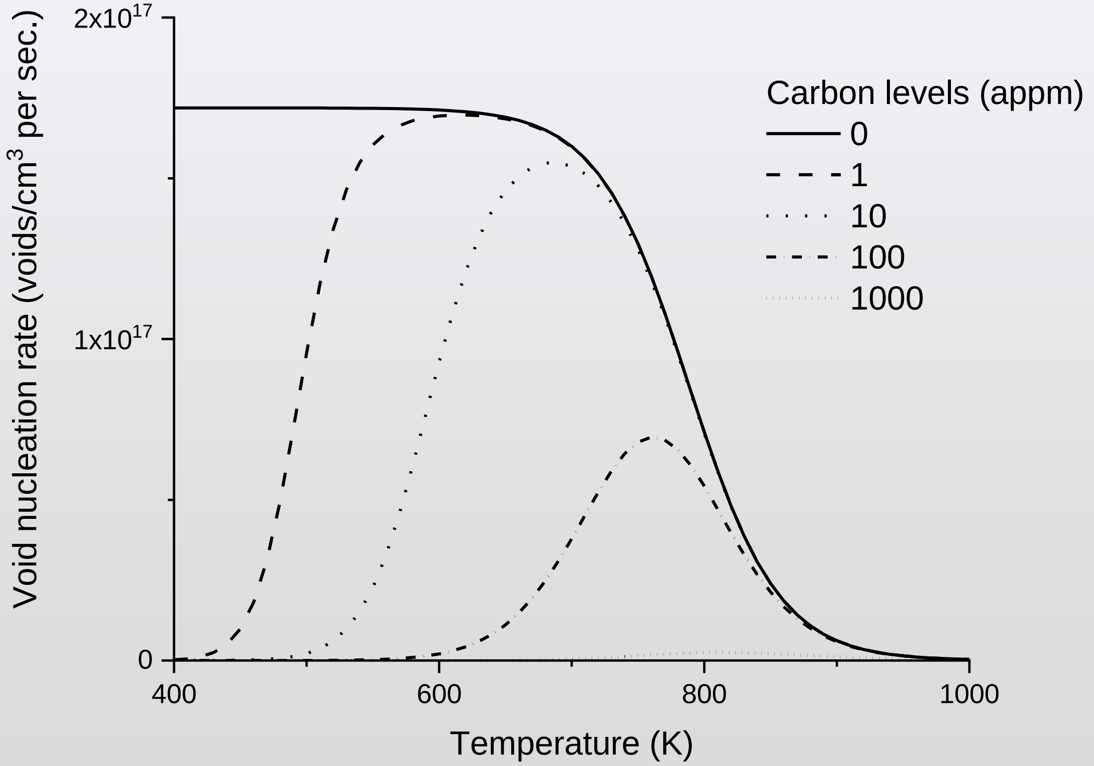

Summary

- Irradiation-induced swelling is much less in AM 316L.
- Out of many possible mechanisms yet to be studied, the calculations of void nucleation show that the steady rates of void nucleation are highly sensitive to carbon.
- Even a seemingly negligible carbon concentration, as low as a few appm, can dramatically reduce the nucleation rates and narrow the temperature window for nucleation.
- The study highlights the importance of impurity control in AM processing and also suggests one potential advantage of AM alloys for excellent swelling resistance.

ACKNOWLEGEMENTS

This material is based upon work supported by the Department of Energy / National Nuclear Security Administration under Award Number(s) DE-NA0003921.